A

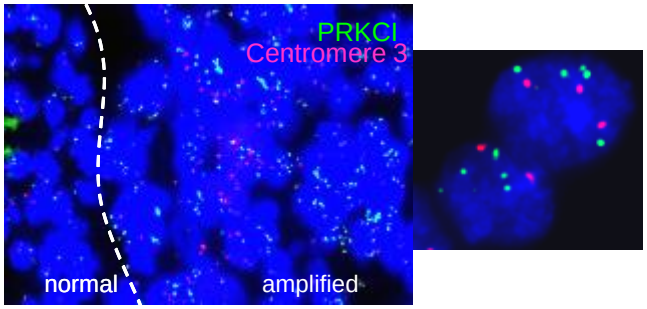

Ovary	Primary	Serous papillary adenocarcinoma	31	14 (45.2%)
		Mucinous papillary adenocarcinoma	5	0
		Endometrial carcinoma	2	0
	Metastatic adenocarcinoma		1	0
Lymph node	Metastatic serous papillary carcinoma		7	0

B

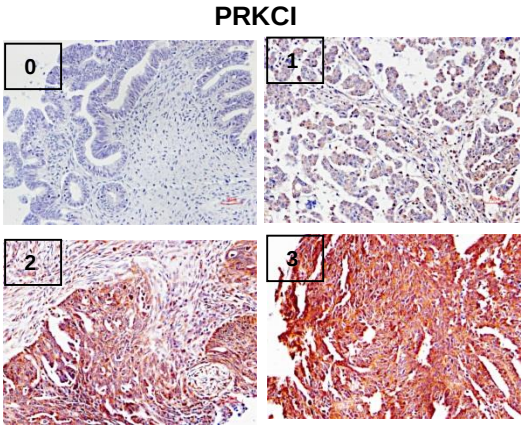

TMA representative scores

C

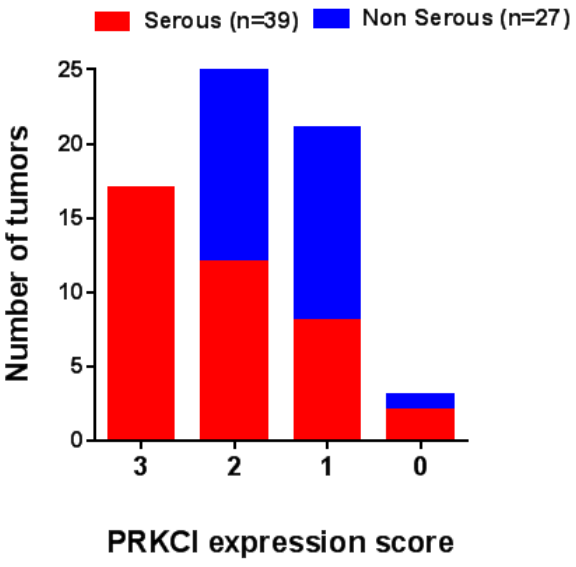

D

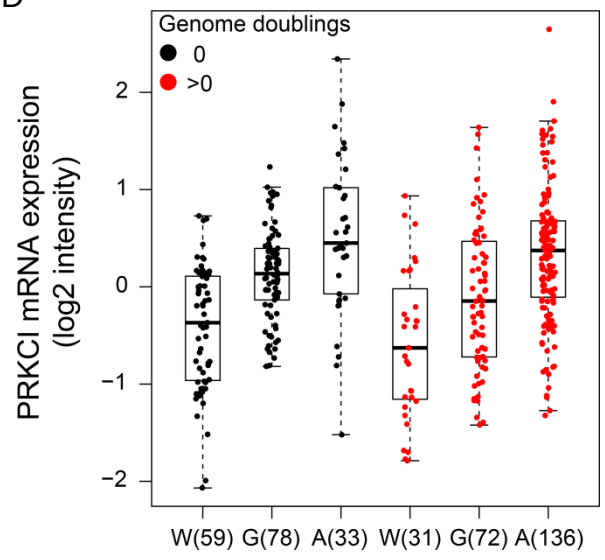

A

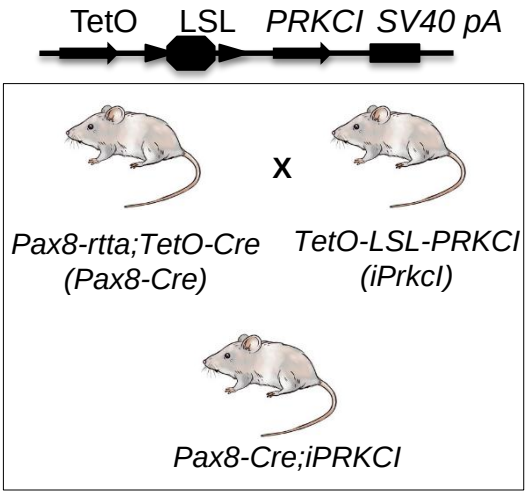
TetO
LSL
PRKCI
SV40 pA
X
Pax8-rtta;TetO-Cre
(Pax8-Cre)
TetO-LSL-PRKCI
(iPrkcI)
Pax8-Cre;iPRKCI

B

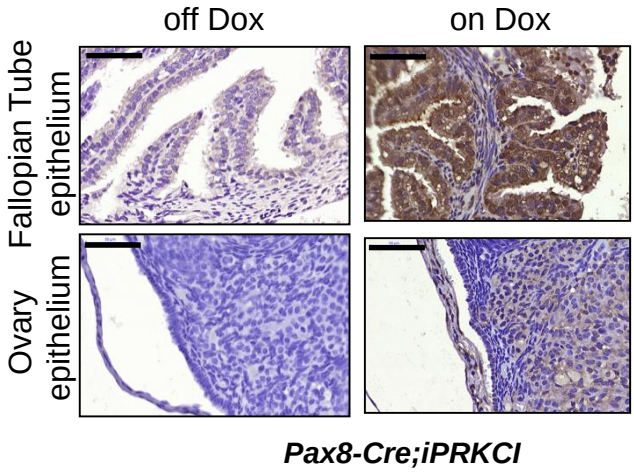
off Dox
on Dox
Fallopian Tube epithelium
Ovary epithelium
Pax8-Cre;iPRKCI

C

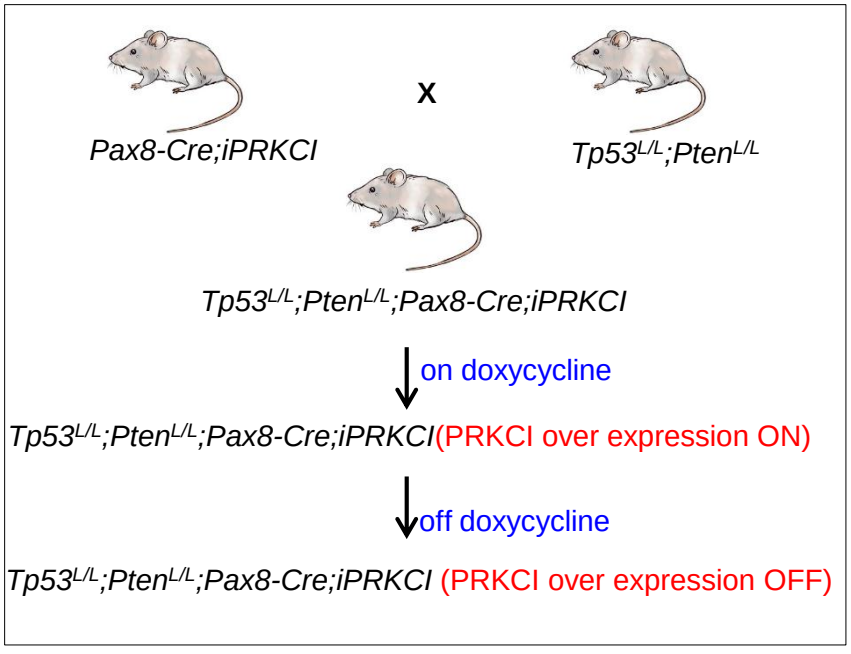
X
Pax8-Cre;iPRKCI
Tp53L/L;PtenL/L
Tp53L/L;PtenL/L;Pax8-Cre;iPRKCI
on doxycycline
Tp53L/L;PtenL/L;Pax8-Cre;iPRKCI(PRKCI over expression ON)
off doxycycline
Tp53L/L;PtenL/L;Pax8-Cre;iPRKCI (PRKCI over expression OFF)

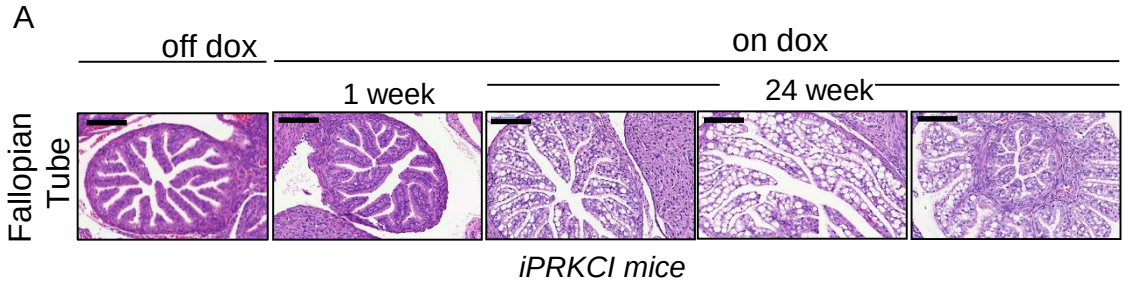
A
off dox
on dox
1 week
24 week
Fallopian Tube
iPRKCI mice

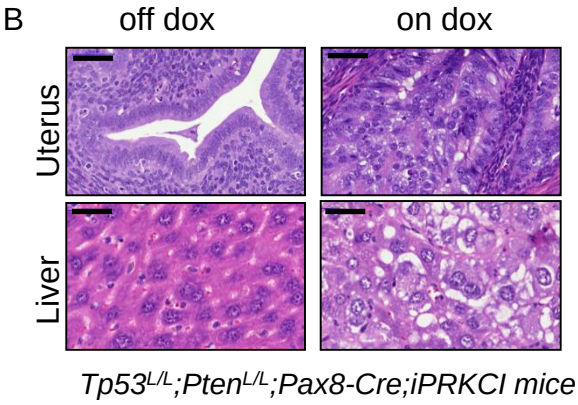
B
off dox
on dox
Uterus
Liver
Tp53L/L;PtenL/L;Pax8-Cre;iPRKCI mice

Sarkar_Fig S4.

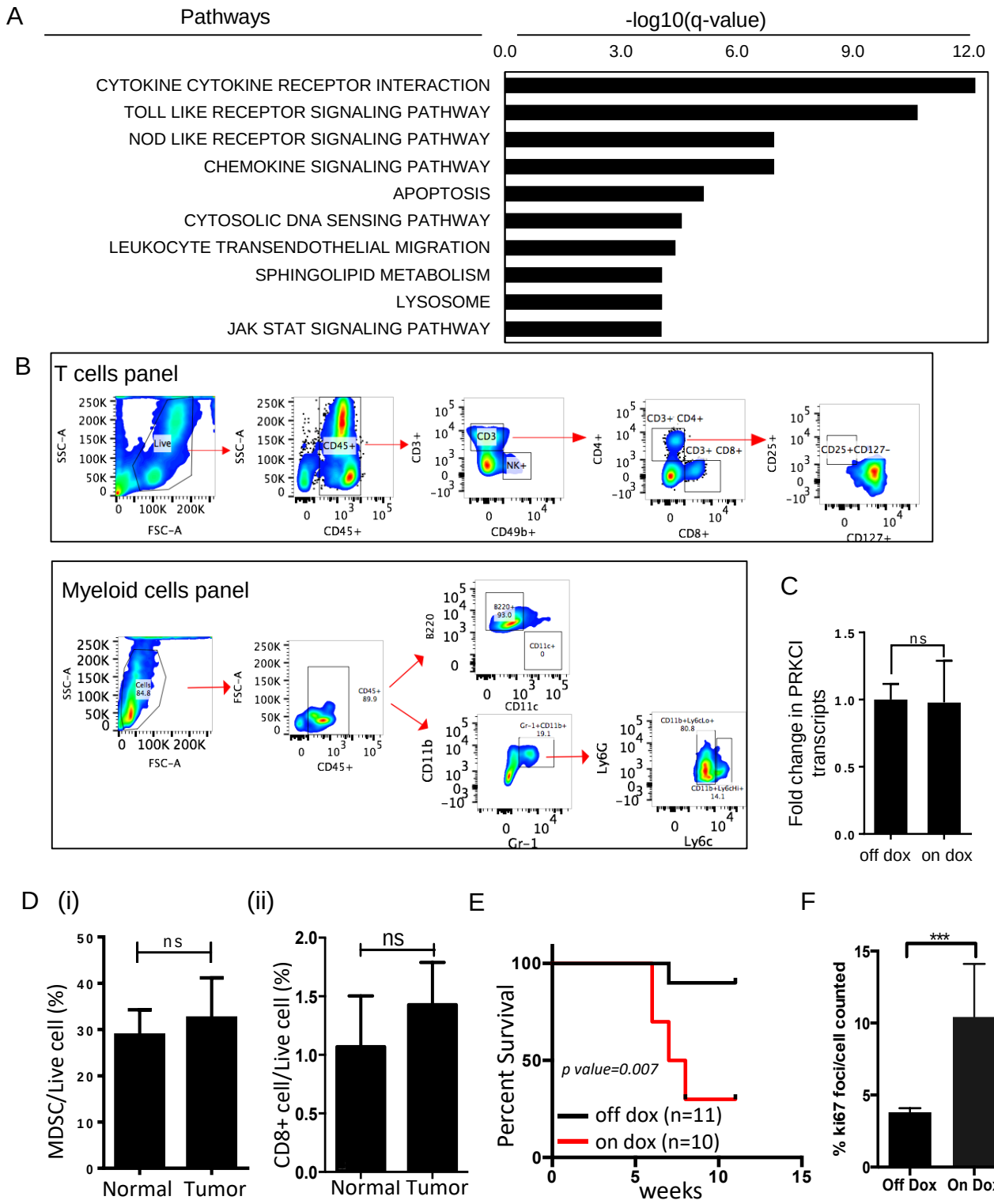

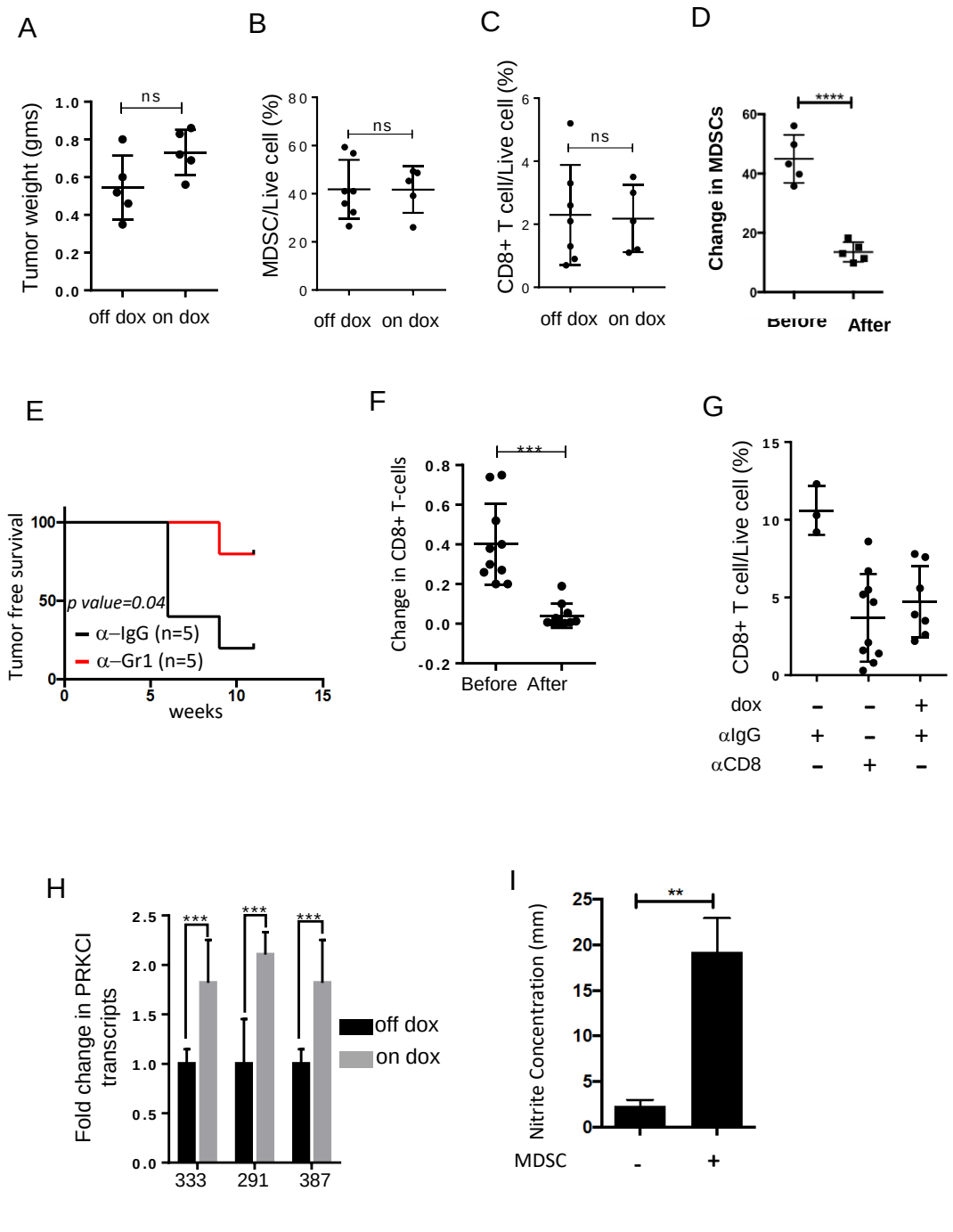
A
Tumor weight (gms)
ns
off dox on dox
B
MDSC/Live cell (%)
ns
off dox on dox
C
CD8+ T cell/Live cell (%)
ns
off dox on dox
D
Change in MDSCs
****
Before After
E
Tumor free survival
p value=0.04
α–IgG (n=5)
α–Gr1 (n=5)
weeks
F
Change in CD8+ T-cells
***
Before After
G
CD8+ T cell/Live cell (%)
dox
αIgG
αCD8
H
Fold change in PRKCI transcripts
***
off dox
on dox
333
291
387
I
Nitrite Concentration (mm)
**
MDSC

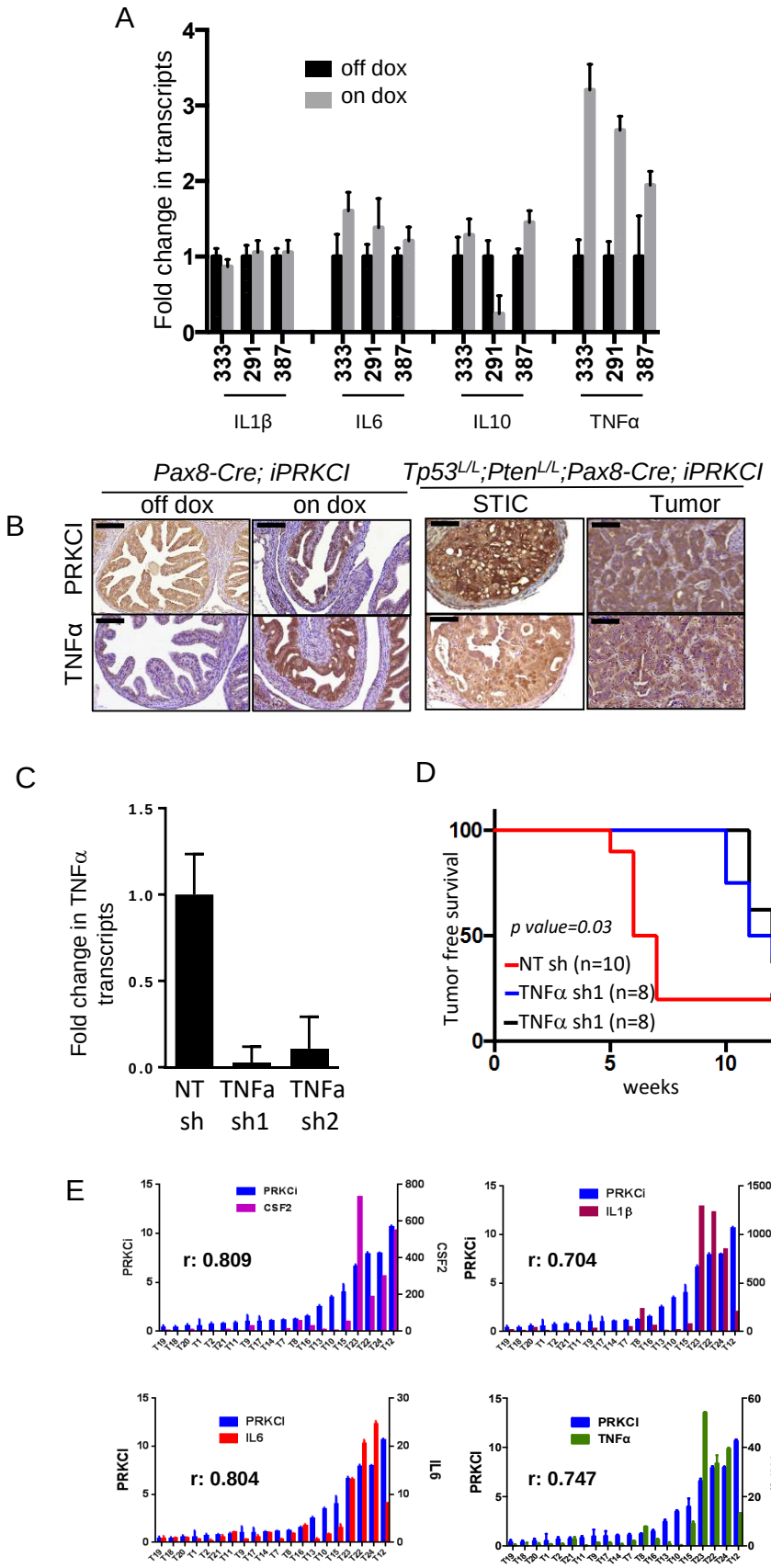
A
Fold change in transcripts
off dox
on dox
333
291
387
IL1β
IL6
IL10
TNFα
B
Pax8-Cre; iPRKCI
Tp53L/L;PtenL/L;Pax8-Cre; iPRKCI
off dox
on dox
STIC
Tumor
PRKCI
TNFα
C
Fold change in TNFα transcripts
NT sh
TNFa sh1
TNFa sh2
D
Tumor free survival
p value=0.03
NT sh (n=10)
TNFα sh1 (n=8)
TNFα sh1 (n=8)
weeks
E
PRKCI
CSF2
r: 0.809
IL1β
r: 0.704
IL6
r: 0.804
TNFα
r: 0.747

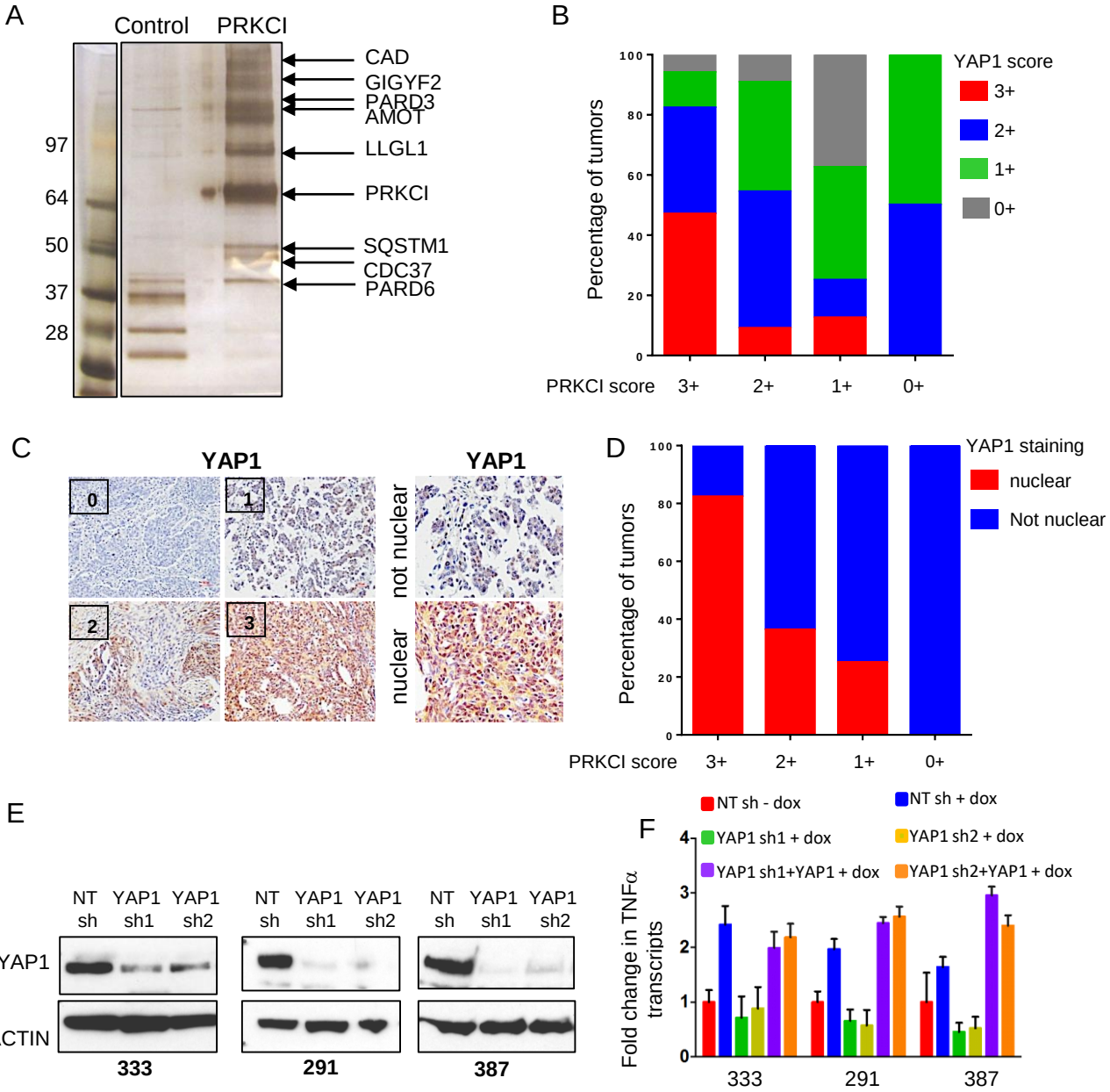
A
Control
PRKCI
CAD
GIGYF2
PARD3
AMOT
LLGL1
PRKCI
SQSTM1
CDC37
PARD6
97
64
50
37
28
B
Percentage of tumors
YAP1 score
3+
2+
1+
0+
PRKCI score
C
YAP1
YAP1
not nuclear
nuclear
D
YAP1 staining
nuclear
Not nuclear
Percentage of tumors
PRKCI score
E
NT sh
YAP1 sh1
YAP1 sh2
YAP1
ACTIN
333
291
387
F
NT sh - dox
NT sh + dox
YAP1 sh1 + dox
YAP1 sh2 + dox
YAP1 sh1+YAP1 + dox
YAP1 sh2+YAP1 + dox
Fold change in TNFα transcripts

Supplementary Figure Legends

Figure S1. PRKCI gene is amplified and overexpressed in serous ovarian carcinoma. (A) FISH analysis of a cohort of ovarian tumor samples reveal increased PRKCI DNA copy (green) in serous subtype but not in mucinous or endometrial subtype. Table represents total sample number and positive samples. Red marks chromosome 3. (B-C) PRKCI protein expression determined by immunohistochemistry in ovarian tumor tissue microarray (TMA) reveals higher levels of PRKCI expression in serous ovarian tumors. Manual blinded scoring of TMA done with 0, 1, 2 or 3 scores depending on expression level. (B) Representative scores of PRKCI expression in ovarian serous tumors. (C) Quantification of scoring of PRKCI expression in ovarian tumor tissue array (n=66) reveals highest expression in serous subtype. (D) PRKCI mRNA expression shows concordant increase with the gain of an additional DNA copy in both genome duplicated samples and non-duplicated samples (W: wild type; G: gain and A: amplification of more than one copy). Sizes of the cohort are listed in the axis label.

Figure S2. Strategy for generating transgenic PRKCI driven mouse model. (A) Schematic representation of strategy used to generate doxycycline inducible PRKCI expression. *Pax8* promoter driven *rtta* mice is crossed with *TetO-Cre* and *iPRKCI* mice to drive expression of PRKCI in PAX8 positive cells. (B) Immuno-staining for PRKCI in fallopian tube epithelium of *Pax8-Cre;iPRKCI* mice show increased PRKCI expression upon treatment with doxycycline for 4 weeks post weaning. (C) Schematic representation of cross between conditional $Tp53^{L/L};Pten^{L/L}$ alleles and *Pax8-Cre;iPRKCI* mice to generate experimental mice cohort.

Figure S3. PRKCI drives tumor formation in liver of *Tp53$^{L/L}$;Pten$^{L/L}$;Pax8-Cre;iPRKCI* mice. (A) H&E staining showing morphological changes in the fallopian tube in *Pax8-Cre;iPRKCI* mice upon extended PRKCI expression. (B) H&E staining showing morphological abnormalities in the liver and uterus of *Tp53$^{L/L}$;Pten$^{L/L}$;Pax8-Cre;iPRKCI* (on dox) mice compared to mice not treated with doxycycline.

Figure S4. PRKCI driven tumors express immune response regulating genes. (A) Gene set analysis of transcriptomes of *Tp53$^{L/L}$;Pten$^{L/L}$;Pax8-Cre;iPRKCI* (on dox) tumors compared to normal fallopian tube from wild type mice treated with doxycycline show immune pathways to be most affected. (B) Gating scheme to identify MDSC and T-cells by flow cytometry. (C) CD8+ T-cells isolated from spleen of *Pax8-Cre;iPRKCI* mice show no change in PRKCI transcript levels with doxycycline. (D) Immune profiling shows no change in (i) MDSC and (ii) CD8+ T-cells in tumors grouped depending on liver morphology. (E) Kaplan Meier plot showing decreased tumor free survival in mice injected with 333 cells and treated with doxycycline compared to untreated mice. (F) Plot showing ki-67 foci in doxycycline on and off (6 different field of view was calculated for each tumor with 3 tumors for each category).

Figure S5. PRKCI overexpression promotes immune suppressive environment in tumors. (A) Plot showing no significant change in tumor weight between on and off doxycycline in mice injected with 333 cells. The mice were initially kept on doxycycline for establishment of tumor and then one cohort taken off doxycycline treatment for 10 days. (B-C) Plot showing doxycycline treatment has no significant change on (B) MDSCs (C) CD8+ T-cells infiltration when PRKCI is overexpressed in 333 cells. (D) Fold change in MDSCs in peripheral blood after α-Gr1 antibody treatment in doxycycline treated mice.

(E) Tumor free survival of mice injected with α-Gr1 antibody. (F) Fold change in CD8+ T -cells in peripheral blood after α-CD8 antibody treatment in doxycycline untreated mice. (G) CD8+ T-cell infiltration in mice treated with α-CD8 antibody. (H) Fold change in PRKCI expression upon doxycycline treatment of tumor derived cell lines. (I) Supernatant from T-cells from OT1 mouse incubated with or without MDSCs are analyzed for nitric oxide production by assaying nitrate in the media.

Figure S6. PRKCI regulates expression of TNFα. (A) Quantitative RT-PCR for IL1β, IL6, IL10 and TNFα. (B) Immuno-staining showing doxycycline treatment increased TNFα in fallopian tube epithelial cells of *Pax8-Cre;iPRKCI* mice and *Tp53$^{L/L}$;Pten$^{L/L}$;Pax8-Cre;iPRKCI* (on dox) tumors. Scale bar represents 20mm for TNFα and PRKCI. (C) RT-PCR showing TNFα knockdown in 333-PRKCI cells. (D) Tumor free survival of mice injected with 333-PRKCI cells expressing TNFα or control shRNA. (E) Quantitative RT-PCR for cytokines IL6, IL1β, TNFα and CSF2 mRNA expression in relation to PRKCI mRNA expression in ovarian tumor samples. Data were normalized to sample T17; bars are mean +/- SD.

Figure S7. PRKCI regulates YAP1 levels and its activity. (A) OVCAR8 cells were engineered to express 3XFlag-6XHis-PRKCi or control vector. PRKCI immunoprecipitated by affinity purification sequentially using Flag M2 beads followed by Ni-beads. Proteins were run on SDS PAGE and bands visualized using silver stain. (B) Graphical presentation showing association of YAP1 and PRKCI staining intensity scores in serous ovarian tumors (n=38). (C) Representative images for scoring intensity of YAP1 nuclear vs. non-nuclear YAP1 in ovarian serous tumors. (D) Graphical presentation showing association of PRKCI and nuclear-YAP1 scores in serous ovarian tumors (n=38)

reveals mostly nuclear YAP1 at highest PRKCI expression. (E) Western blot showing YAP1 knockdown in 333, 291 and 387 cells with YAP1 shRNA. (F) Quantitative RT-PCR shows reduced expression of TNFα expression upon YAP1 knockdown in *Tp53$^{L/L}$;Pten$^{L/L}$;Pax8-Cre;iPRKCI* tumor derived cell lines.